INTERNATIONAL ATOMIC ENERGY AGENCY
UNITED NATIONS EDUCATIONAL, SCIENTIFIC AND CULTURAL ORGANIZATION

INTERNATIONAL CENTRE FOR THEORETICAL PHYSICS
34100 TRIESTE (ITALY) - P.O.B. 586 - MIRAMARE - STRADA COSTIERA 11 - TELEPHONE: 2240-1
CABLE: CENTRATOM - TELEX 460392-1

SMR.380/19

COLLEGE ON THEORETICAL AND EXPERIMENTAL RADIOPROPAGATION SCIENCE

6 - 24 February 1989

LECTURE 3: MAGNETOIONIC THEORY - II

P.A. BRADLEY

Rutherford Appleton Laboratory, U.K.

Lecture 3: Magnetoionic theory - II

P A Bradley

Rutherford Appleton Laboratory, UK

2 WAVE CHARACTERISATION

2.1 Full-Wave Methods

At low and especially at very low frequencies the medium through which the wave propagates can vary appreciably in the space of one wavelength. Thus, the conventional ray optics used to describe the propagation of high-frequency radio waves in the ionosphere no longer applies. Full-wave solutions become necessary in which the wave fields are calculated at many points in the course of one wavelength. A number of full-wave methods have been developed for calculating the reflection properties of the lower ionosphere at low and very low frequencies.

In the usual methods of calculation(1) the differential equations satisfying some field component of the wave are first formulated. Solutions are then obtained at great heights, well above the reflection levels, and these correspond to purely upgoing waves. Connection formulae are applied to obtain solutions down through the ionosphere. Below the base of the ionosphere these are separated out into upgoing and downgoing waves. The associated reflection coefficients are calculated, which depend on the polarisation of the incident wave. In general, the incident and reflected waves do not have the same polarisation and the reflection properties must be completely specified by the four parameters ${}_{\parallel}R_{\parallel}$, ${}_{\parallel}R_{\perp}$, ${}_{\perp}R_{\perp}$, ${}_{\perp}R_{\parallel}$.

Numerical methods for full-wave solution of the wave equations have been extensively discussed in the literature, the method of Pitteway (2) receiving considerable use. In this method, fourth-degree polynomials are fitted to the solutions of the differential equations by calculating four separate sets of derivatives at each height. The process is then repeated towards the base of the ionosphere until free space is reached. Here the solution is separated into upgoing and downgoing components and the reflection and conversion coefficients determined. Care must be taken during the numerical integration to ensure that the two solutions remain independent; suitable constraints are applied at each integration step.

Various other numerical full-wave analyses have been developed (3, 4). These all enable the complex reflection and conversion coefficients to be determined for any given height distribution of electron concentration and collision frequency. Parameters such as the wave frequency, path azimuth, angle of incidence, and magnetic-field intensity and dip are easily varied. Thus the reflection parameters of VLF and LF waves can be calculated for conditions representative of any time-of-day, season and at any geographical location. Clearly this technique provides a powerful tool in the design and operation of VLF/LF radio-wave systems.

2.2 Waveguide-Mode Propagation

When propagation takes place to great distances, further complications occur in that a large number of raypaths can be established between the transmitter and receiver. This situation can conveniently be represented in terms of waveguide-mode propagation, where the Earth and the ionosphere form the walls of a spherical waveguide. A combination of full-wave and waveguide-mode analyses enables the phase, amplitude and polarisation of VLF and LF waves propagated to great distances to be

The theory of VLF radio-wave propagation has been extensively developed by Budden (1), Wait (5), Galejs (6) and Pappert (7). At these frequencies for long-range propagation the Earth behaves like a good electrical conductor with a reflection coefficient approaching + 1, while the ionosphere has a reflection coeffient approaching - 1. It is convenient thus to treat the Earth and the ionosphere as the two boundaries of a spherical waveguide and to consider propagation to great distances in terms of waveguide modes.

A vertical antenna situated on the surface of the Earth will excite transverse magnetic waveguide modes. For each mode there are three parameters which govern its characteristics: the attenuation rate, the phase velocity and the excitation factor, which is the ratio of the power launched into the Earth-ionosphere waveguide to that which would have been launched into an ideal flat waveguide with perfectly conducting boundaries. Wait and Spies (8) have presented numerical values of these parameters for propagation over sea water. These show that mode 2 suffers more attenuation than mode 1 both by day and night, differences being more marked for the lower frequencies (Fig. 1). Also, that the difference in phase velocity between night and day for mode 1 is larger at the lower frequencies (Fig. 2). This indicates that at large distances from a transmitter where mode 1 would be the dominant mode both by day and night the diurnal phase delay pattern should increase in magnitude linearly with distance and have a larger magnitude the lower the frequency. Both these features are borne out by the experimental results. For distances closer to a transmitter the effects of the second mode should become more marked. This is especially so at the higher frequencies since at these frequencies, as may be seen from Fig. 3, the second mode is more easily excited in the waveguide; at 20 kHz for example the excitation factor for mode 2 is some 10-15 dB greater than for mode 1 under night conditions while at 10 kHz they are more or less equally excited.

Fig. 4 shows a theoretical estimate of the diurnal phase delay variation at 16 kHz based upon the waveguide model stated above, where the reference heights for day and night are 75 and 88 km respectively. This theoretical curve illustrates the effect of the second mode in causing the distance variation to depart from a linear form. Of special interest is the manner in which the theoretical curve fits the experimental data for distances in the 1000-3000 km range. A corresponding curve for 10 kHz is also shown, from which it is evident that the effect of the second mode is much smaller, due to its larger attenuation rate under day conditions and the larger excitation factor of mode 1 at this frequency compared to 16 kHz. Theoretical advances by Galejs (6) and Pappert (7) now enable an arbitrary ionospheric profile together with an arbitrary terrestrial magnetic field to be incorporated in the waveguide model. With an appropriate choice of lower ionosphere model these permit better agreement to be achieved between theory and experiment, (Bain and Harrison, 9).

2.3 Wave-Hop Theory

The waveguide mode theory of propagation is useful when only a few modes need to be considered. This holds for frequencies less than about 30 kHz. At higher frequencies it is more appropriate to view propagation in terms of wavehops (Berry and Chrisman, 10), although Johler (11) has developed a theory covering the frequency range from VLF to MF which considers propagation in terms of spherical wave functions.

In the wavehop theory, the full-wave solution for propagation between a spherical Earth and a concentric ionosphere can be expanded into a series of complex integrals. If these integrals are replaced by their saddle-point approximations, the series can be identified as the ray hop

series of geometric optics, and thus these integrals are called wavehops. The saddle-point approximation is inadequate near and beyond the caustic and in this area the wavehops can be evaluated by numerical integration or by summing a residue series. Berry and Chrisman (10) represent the series in the form

$$E = E_g + \sum R_j I_j \qquad (1)$$

where E_g is the groundwave and R_j is the ionospheric reflection coefficient of the j'th wavehop. The path integral I_j takes into account ground conductivity, path length, reflection height and Earth curvature.

Raypath elevation angles ψ are determined on the basis of assumed mirror reflection from heights of 70 km by day and 90 km by night. Allowances for the effects of atmospheric refraction may be included. The vertical component of electric field E_o radiated from a short vertical electric dipole may be written as

$$E_o = 300 \sqrt{P} \text{ mV/m at a range of 1 km} \qquad (2)$$

where P is the radiated power in kW. The field strength of the downcoming skywave before reflection at the ground in the vicinity of the receiving antenna (from a single wavehop) E_d is given by

$$E_d = \frac{E_o}{L} \cos\psi \cdot {}_{//}R_{//} \cdot D F_T \text{ mV/m} \qquad (3)$$

where

L = skywave path length in km

${}_{//}R_{//}$ = ionospheric reflection coefficient which gives the ratio of the electric-field components parallel to the plane of incidence

D = ionospheric focusing factor

and F_T = transmitting antenna factor.

3 PROPAGATION EFFECTS AT VLF AND LF

3.1 General

VLF/LF radio waves are reflected from the lowest part of the ionosphere and extensive studies undertaken in the late 1930's by a group at Cambridge, England, showed that apart from sunrise and sunset periods, the reflecting region was remarkably stable in both phase and amplitude. Furthermore, little attenuation of the waves occurred during the reflection process. In this frequency range, at distances beyond which the ground wave becomes too weak to be useful, i.e between 500 and 1500 km depending on frequency and earth-surface conditions, propagation continues between the earth and the lower boundary of the ionosphere and is characterised by good reliability and stability. For a given radiated power, increased field strength is obtained with decreasing frequency down to 10-20 kHz and the diurnal, seasonal and solar-cycle changes become smaller.

In the presence of a reflecting layer, interference may be expected between the direct ground wave and the reflected signal. Hollingsworth (12), using a frequency of 21.4 kHz, demonstrated the interference as a series of well defined maxima and minima of signal strength with increasing distance from the transmitter. From these observations he deduced an equivalent height of 75 km for the reflecting layer for summer midday conditions. Propagation anomalies associated with solar and magnetic disturbances were soon noted as indicated by Espenschied et al. (13) and Austin (14). The influence of the Earth's magnetic field was appreciated at this early stage and Round et al. (15) noted that propagation from East to West was more difficult than from North to South.

3.2 Undisturbed Conditions

3.2.1 VLF amplitude and phase measurements. Measured propagation data are consistent with groundwave and skywave interference patterns out to a range of around 1000 km, depending on frequency. At larger distances changes are associated with variations in the dominant skywave mode. Diurnal and seasonal variations can be related to changes in layer reflecting heights.

Fig. 5 compares the diurnal variations of amplitude and phase recorded at 14.7 kHz and 18.6 kHz on a 680 km path between Cutler, Maine and Ottawa, Canada using an in-plane loop responding to the total incident field. The marked difference between the two sets of recordings clearly demonstrates that the phase relationship between ground and sky waves is different in the two cases. The marked minima in field strength before sunrise and after sunset at 18.6 kHz are assumed to be due to the ground and sky waves being in anti-phase at these times, whereas at 14.7 kHz the phase relation between ground and sky waves is not well established by the recordings. Clearly at 14.7 kHz the sky and ground waves are in the anti-phase quadrant during the night and in the co-phase quadrant by day, thereby accounting for the relative weak field intensities during the night and much larger amplitudes during the day. These results illustrate how, within the interference zone, either day or night amplitudes may be the larger, depending on frequency and transmission distance.

The very marked changes which occur in the diurnal pattern of phase variation of the total field have been summarised by Belrose (16) and are reproduced in Fig. 6. It is evident from the Figure that the greatest phase changes occur at sunrise and sunset and these phase transitions have been extensively studied (17-20). In general the sunrise/sunset behaviour has been explained in terms of a change in the dominant waveguide mode as the reflecting layer height varies. At short distances, say less than 200 km, there is little diurnal variation, since the wave received is mainly a ground wave. At distances of 700 km the ground and skywave signals can be approximately equal during the twilight transitions, as already noted for the Cutler-Ottawa path. The diurnal phase variation for the Rugby-Rome path, 16 kHz propagated to 1500 km, is roughly trapezoidal in shape, as also are the results on paths greater than 3000 km. The rather simple pattern is however deceptive, since the daily variations can be sometimes more complex, indicating the presence of more than one mode of propagation. The total phase change from night to day rises as distance increases. For transmission distances between 2000-2500 km, the change of phase from night to day is very small, although rapid oscillatory phase variations tend to occur in these periods, accompanied by corresponding amplitude changes, indicating the presence of a second ionospheric mode during the hours of darkness. In the case of the Rugby-Idris path, 16 kHz at 2500 km, the two modes at night apparently have comparable amplitude since the phase variations over say an hour or two can be as large as ±15

microseconds, whereas the random variations during the night for the Rugby-Malta transmission, 16 kHz at 2200 km, are only of the order of a few microseconds.

As the transmission distance is increased, eventually for some particular distance which depends on azimuth, frequency, ionosphere and ground conditions, signal reception over the reciprocal great-circle path is possible. Because of non-reciprocity in east-to-west and west-to-east propagation with westwards attenuations exceeding those for propagation in an easterly direction, the distance where this occurs can be much less than half-way round the Earth. Attenuation rates change with time-of-day and so there is a possibility of both paths being dominant at different times.

Phase and amplitude measurements over long transequatorial paths exhibit variations which can be interpreted in terms of the interference pattern of propagating modes. Some observations show other complicating features. Chilton and Radicella (21) compared the phase and amplitude of 18 kHz waves from Balboa recorded at Boulder, Colorado in the northern hemisphere and Tucuman, Argentina in the southern hemisphere. Although these two propagation paths are essentially the same length, there is a noticeable difference between measured results. The diurnal phase change over the Balboa-Boulder path is markedly larger, and the field strength is significantly lower at Tucuman. These facts, together with a pronounced diurnal variation in amplitude and phase, provide evidence that the reflecting properties of the lower ionosphere are different at low latitudes than at high latitudes.

The very low ground conductivities in polar regions and the particular conditions prevailing at high latitudes, due in part to solar geometry and in part to ionospheric disturbances, lead to special propagation effects. On trans-polar paths, there is no change of phase and amplitude on that fraction of path illuminated by the midnight sun or in continuous darkness during the winter. Blackband (22) has made observations at Farnborough, England on 18.6 kHz of transmissions from Seattle. The path crosses and recrosses the effective Artic circle and therefore during the polar summer and winter the received phase changes only when the parts of the paths at the two end points are in twilight. Thus two phase humps are recorded, separated by some 5 hours. On another path, with the receiver located at Bodo, Norway above the Arctic circle, only the part of the path on the transmitter side underwent a diurnal change in midsummer and midwinter, leading to a single phase hump.

The Seattle-Farnborough path traverses Greenland which is ice covered much of the time. This results in a considerable increase in attenuation in the Earth-ionosphere waveguide at night, and therefore in an unusually large diurnal change in amplitude and phase. Attenuations of 22 dB/1000 km by night and 1.3 dB/1000 km by day have been reported for paths which traverse Greenland. It should be noted that not only are these attenuations very great, but the diurnal changes are in the opposite sense to those found on typical mixed land and sea paths, where values of 2 and 3 dB/1000 km apply by night and day respectively. It has been found very difficult, for example, to receive GBR (Rugby) 16 kHz at Fairbanks or Anchorage, Alaska, particularly in summer, because the path traverses diagonally the widest section of Greenland, whereas GBR can be received reliably at Barrow, Alaska, and elsewhere at greater distances for paths which do not traverse the Arctic or Antarctic icecaps.

3.2.2 LF amplitude and phase measurements. As at VLF, short-range signals at LF also display interference patterns between the ground and sky waves. Measurements may be made at a fixed location noting the pattern traced out due to change of phase of the sky wave because of path length variations as the height of reflection alters from night to day (Fig. 7). Alternatively, measurements may be made in an aircraft flying radially from a transmitter. Fig. 8 shows the Hollingsworth interference patterns obtained by Bracewell et al. (23) in this latter way at 85 and 127.5 kHz on the path from Copenhagen to Farnborough.

The absorption of LF waves is found to be considerably greater than for VLF waves. Bracewell et al. (23) studied the frequency dependence of the ionospheric reflection coefficient. Below 20 kHz, the variation from night to day is from a coefficient of 0.50 to about 0.10 in summer, whereas, at 100 kHz for the same conditions, it varies from 0.20 to a value less than 0.0001. During winter daytime the medium is a much better reflector, giving reflection coefficients of 0.35 (<20 kHz) and 0.03 (~100 kHz). As the path becomes more oblique the reflection coefficient increases to a maximum at grazing incidence. Detailed investigations of the propagation of LF waves to distances of up to 1000 km have been undertaken by a group at Kuhlungsborn, East Germany. These experiments indicated that the behaviour of radio waves in the 100 to 700 kHz band can be quite different to that at lower frequencies. Marked fading effects were observed at night and these propagation paths were also sensitive to transient disturbances in the D-region. A review of these experiments has been given by Lauter (24). The maximum effective range of LF signals by day is 2000 km or less.

LF waves propagated to distances of 400-1000 km in Europe are reflected from apparent heights which match those during the day for VLF waves steeply incident on the ionosphere. When these waves propagate over shorter paths (say less than 300 km) they are reflected from somewhat greater heights of 80-85 km by day and 90-100 km by night.

Phase measurements of LF waves propagated over paths in Canada at somewhat higher magnetic latitudes reveal clear differences in diurnal variation from these mid-European observations. This must be due to a difference in the diurnal behaviour of the ionospheric reflecting layers, presumably related to the differing magnetic latitudes. The changeover from cosine to trapezoidal phase pattern is therefore not only a function of frequency and range, but is also dependent on the latitude of the transmission path.

When an ionospheric wave is transmitted over distances of 100-300 km, UK results show that the downcoming signal for frequencies up to 150 kHz is approximately circularly polarised with an anticlockwise rotation viewed along the direction of propagation. It is linearly polarised for greater distances. Theory indicates that polarisation depends on magnetic dip and direction of propagation with respect to the direction of the Earth's magnetic field.

In addition to the amplitude features discussed, fading also occurs. This arises from changes in reflection heights, changes in reflection coefficients, focusing or defocusing by the ionosphere and interference between the various waves which reach the receiver. The order of size of the first Fresnel zone is several hundred kilometres at LF and proportionately greater at VLF, so it is not surprising that the ionospheric parameters within this region are non-stationary. Daytime sky-wave signals appear to be relatively steady consistent with a sppecular-like reflection, particularly at the lower frequencies, but they display significant fading near the upper end of the LF band. At all frequencies the skywave field is less regular during the night time. Short-term amplitude-probability distributions are log-normal, consistent with a random component superimposed on a component subject to bodily movement of the reflection height. Bowhill (25) has pointed out that the fading of long waves seems to be made up of two components with quite

different amplitudes and fading speeds. The fading of the dominant component, which is relatively independent of frequency, has a substantially constant quasi-period of about 7 minutes. This is readily evident at steep incidence, but difficult to recognise at oblique incidence, and at the lower frequencies. Superimposed on this slow fade is a smaller component whose fading speed is more rapid. The fading speed of this component varies somewhat from time to time, but when simultaneous observations are made at a number of frequencies, it is found to vary with the equivalent frequency.

3.3 Disturbed Conditions

The discussion, so far, has been concerned with the normal diurnal changes observed in the propagation characteristics. The lower ionosphere is however sensitive to a number of geophysical disturbances such as those resulting from solar flare and magnetic-storm activity. During flare conditions the solar X-ray flux is enhanced and additional ionisation is produced in the D-region when the path is sunlit. The effective reflection height is decreased by as much as 10 km and a phase advance is noted on short propagation paths (16, 26). The effects usually last from some tens of minutes to an hour or so, with the onset being much more rapid than the recovery. There seems to be little relationship between the size of the phase perturbation and the optical classification of the flare. Sudden ionospheric disturbances of this type lead to associated sudden phase anomalies and sudden field anomalies with different forms, depending on frequency and transmission path length. The forms are particularly variable for the shorter ranges where there is interference with the groundwave.

Perhaps the best known disturbance effects on VLF/LF propagation are those associated with magnetic storms which are believed to be due to precipitation of energetic electrons into the lower ionosphere. During magnetic storms, anomalies are produced in both the phase and amplitude of VLF and LF waves propagated over both short and long paths. These events are of long duration, lasting for up to ten days or more. Unlike solar flare effects which influence a wide region simultaneously, electron precipitation events are more localised in space and time. The disturbance takes the form of irregular variations having quasi-periods of the order of tens of minutes, superimposed on the normal diurnal variation. While the electron precipitation is strongest at auroral latitudes, effects can be detected at lower latitudes where there is a storm after-effect. The main features associated with magnetic storm effects have been summarized by Lauter and Sprenger (27) and Lauter and Knuth (24). These authors note that the sudden commencement of the magnetic storm does not influence the received signal strength. The main phase of the storm produces deep fading at night and this is known as the primary storm effect. No daytime anomalies are noted during the main phase of the storm. For large storms, high absorption sets in 3 or 4 days after storm commencement and continues for several days; this is the so-called storm after effect. Similar behaviour has been noted on VLF signals propagated at steep incidence (16). The phase of the VLF signals is sensitive to the storm and phase advances are noted, particularly at night. For long path VLF propagation, both the night and daytime phase is advanced and the regular day/night transition is displaced.

On high latitude paths, phase and amplitude anomalies are observed during solar cosmic-ray events. The cause of these events, which last for several days, is enhanced ionisation of the D-region by solar protons in the energy range 80-100 MeV which are emitted during solar flares. In general this extra ionisation produces a lowering of the reflection heights of the VLF and LF waves and a corresponding change in the received phase. The nighttime phase is depressed and the diurnal phase variation can disappear entirely. The nighttime amplitude is less than normal but during the day the signal level is normal or even increased. These effects are dependent on the latitude of the propagation path and have been discussed in detail by Lange-Hesse and Rinnert, (28); Ortner et al. (29), and Belrose and Ross (30). Most polar-cap disturbances last for several days.

REFERENCES

1. Budden, K G (1961). Radio waves in the ionosphere, Cambridge University Press.

2. Pitteway, M L V (1965). The numerical calculation of wave fields, reflection coefficients and polarizations for long radio waves in the lower ionosphere - Pt. 1, Phil. Trans. Roy. Soc., A275, 219-241.

3. Altman, C and Cory H (1967). Applications of thin-film optics to very low frequency radio propagation in the ionosphere, Conf. on MF, LF and VLF radio propagation, IEE Conference Pub. 36, 98-105.

4. Inoue, Y and Horowitz S (1966). Numerical solution of full-wave equation with mode coupling, Radio Science, 1, 957-970.

5. Wait, J R (1962). Electromagnetic waves in stratified media, McMillan, New York.

6. Galejs, J (1967). Propagation of VLF waves below anisotropic ionosphere models with a dipping static magnetic field, Radio Science, 2, 1497-1512.

7. Pappert, R A (1968). A numerical study of VLF mode structure and polarization below an anisotropic ionosphere', Radio Science, 3(3), 219-233.

8. Wait, J R and Spies K (1964). Characteristics of the earth-ionosphere wave-guide for VLF radio waves, NBS Technical Note 300.

9. Bain, W C and Harrison M D (1972). Model ionosphere for the D region at summer noon during sunspot maximum, Proc. IEE, 119, 790-796.

10. Berry, L A and Chrisman M E (1965). The path integrals of LF/VLF wave hop theory, Radio Science, 69D(11), 1469-1480.

11. Johler, J R (1970). Spherical wave theory for MF, LF and VLF propagation, Radio Science, 5(12), 1429-1444.

12. Hollingsworth, J (1926). The propagation of radio waves, Jour. IEE, 64, 579-589.

13. Espenschied, L Anderson C N and Bailey A (1926). Transatlantic radio telephone transmission, Proc. IRE, 14, 7-56.

14. Austin, L W (1927). Longwave radio measurements at the Bureau of Standards in 1926 with some comparison of solar activity and radio phenomena, Proc. IRE, 15, 825-836.

15. Round, H J et al. (1925). Report on measurements made on signal strength at great distances during 1922 and 1923 by an expedition sent to Australia, Jour. IEE, 63, 933-1011.

16. Belrose, J S (1968). Low and very low frequency radio-wave propagation, Radio wave propagation, AGARD Lecture Series XXIX, IV-1 to IV-115.

17. Reiker, J (1963). Sunset and sunrise in the ionosphere-effects on the propagation of long waves, J. Res. NBS, 67D, 119-138.

18. Crombie, D D (1964). Periodic fading of VLF signals received over long paths during sunrise and sunset, Radio Science, 68D, 27-34.

19. Walker, D (1965). Phase steps and amplitude fading of VLF signals at dawn and dusk, Radio Science, 69D, 1435-1443.

20. Ries, G (1967). Results concerning the sunrise effects of VLF signals propagated over long paths, Radio Science, 2, 531-538.

21. Chilton, C J and Radicella S M (1965). Differences between transequatorial and middle latitude VLF propagation, Report on equatorial aeronomy, Ed. F. de Mendonca, 33-39.

22. Blackband, W T (1964). Diurnal changes of transmission time in the arctic propagation of VLF waves, Radio Science J. of Res. NBS, 68D, 205-210.

23. Bracewell, R N Budden K G, Ratcliffe J A, Straker T W and Weekes K (1951). The ionospheric propagation of low and very low frequency radio waves over distances less than 1000 km, Proc. IEE, 98, 221-236.

24. Lauter, E A and Knuth R (1967). Precipitation of high energy particles into the upper atmosphere at medium latitudes after magnetic storms, J. Atmos. Terr. Phys., 29, 411-417.

25. Bowhill, S A (1956). The fading of radio waves of frequencies between 16 and 2400 kc/s, J. Atmos. Terr. Phys., 8, 129-145.

26. Weekes, K (1950). The ground interference pattern of very low frequency radio waves, Proc. IEE, 97(III), 100-107.

27. Lauter, E A and Sprenger K (1952). Nocturnal disturbances in the lower ionosphere, Zeif. fur. Met., 6, 161-173.

28. Lange-Hesse, G and Rinnert K (1970). Phase deviations on long distance VLF propagation over high latitudes, Ed. K. Davies, AGARD Conf. Proc. 33, 138-144.

29. Ortner, J, Egeland A and Hultqvist B (1961). A new sporadic layer providing VLF propagation, IRE Trans. AP-8, 621.

30. Belrose, J S and Ross D B (1962). Observations of unusual MF propagation made during polar cap disturbances (PCD) events, J. Phys. Soc. Japan, 1, Suppl. A-II, 126-130.

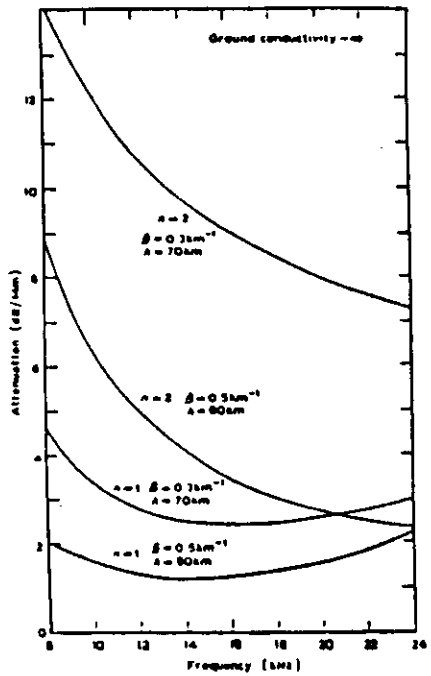

Fig. 1 Calculated attenuation rates for the first and second TM modes as a function of frequency (from Wait and Spies, 8)

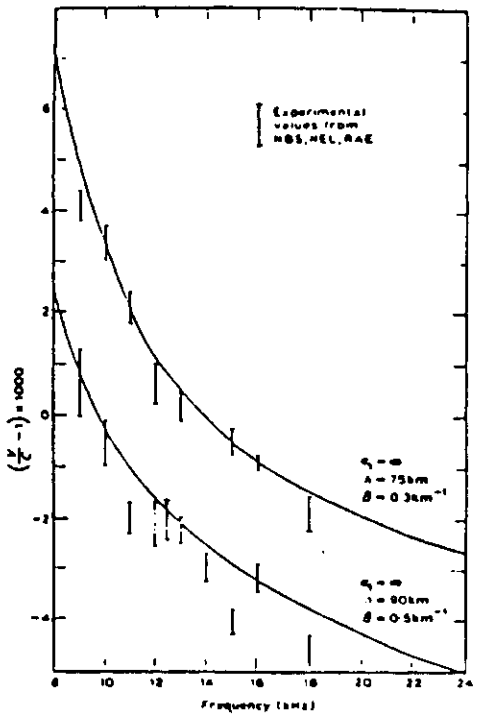

Fig. 2 Comparison of calculated and measured values of the phase velocity parameter (from Wait and Spies, 8)

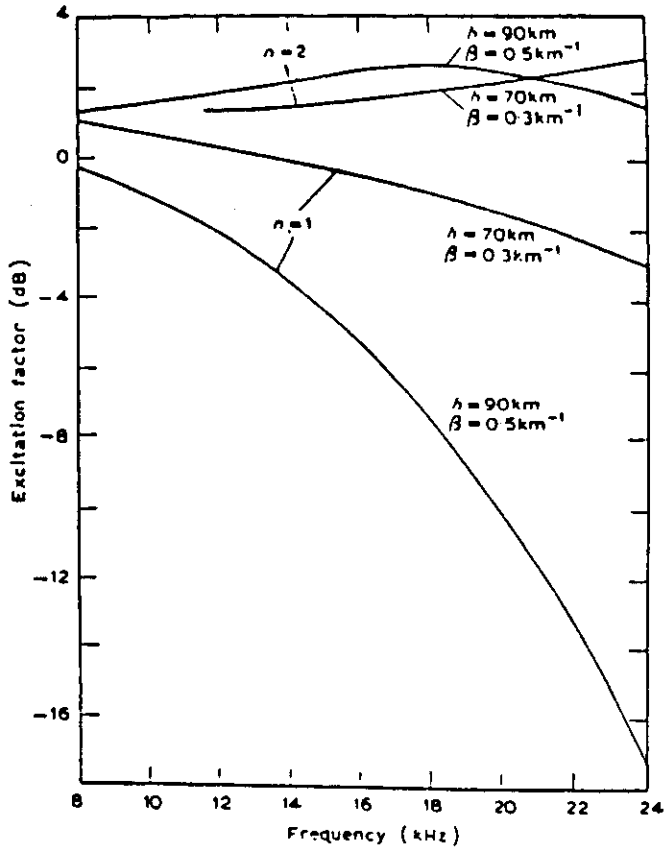

Fig. 3 Calculated excitation factors for day and night conditions (from Wait and Spies, 8)

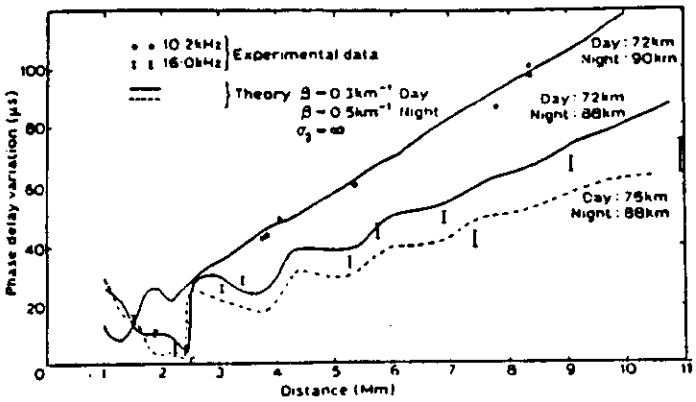

Fig. 4 Dependence of mean night-to-day phase change of 10.2 kHz and 16 kHz signals on range (from Burgess and Jones)

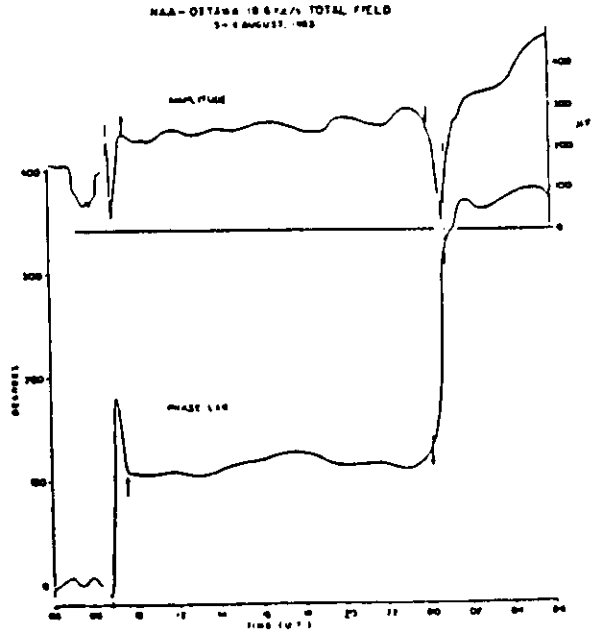

Fig. 5 Amplitude and phase of signals at 13.6 kHz received at Ottawa from Cutler, Maine, range 680 km (from Belrose, **16**)

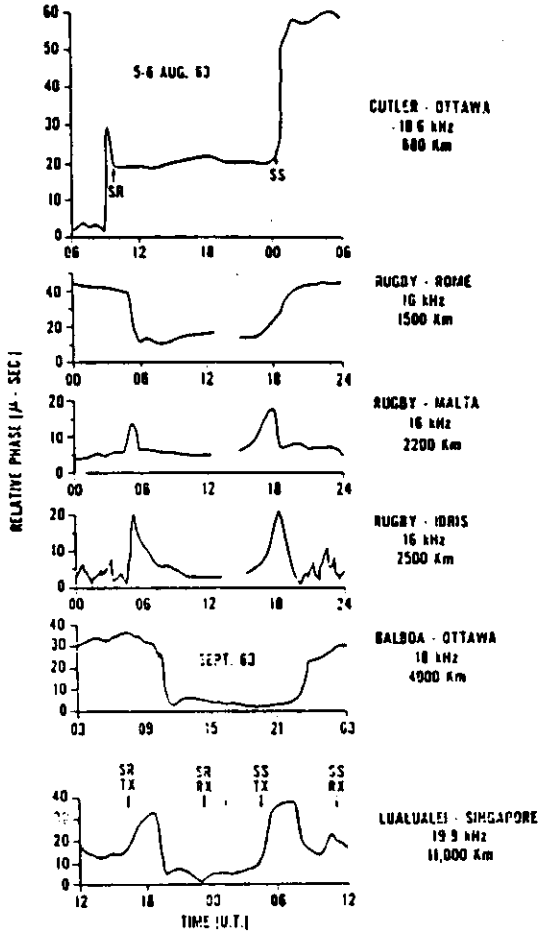

Fig. 6 Diurnal variation of phase lag of VLF signals on paths of different lengths (from Belrose, **16**)

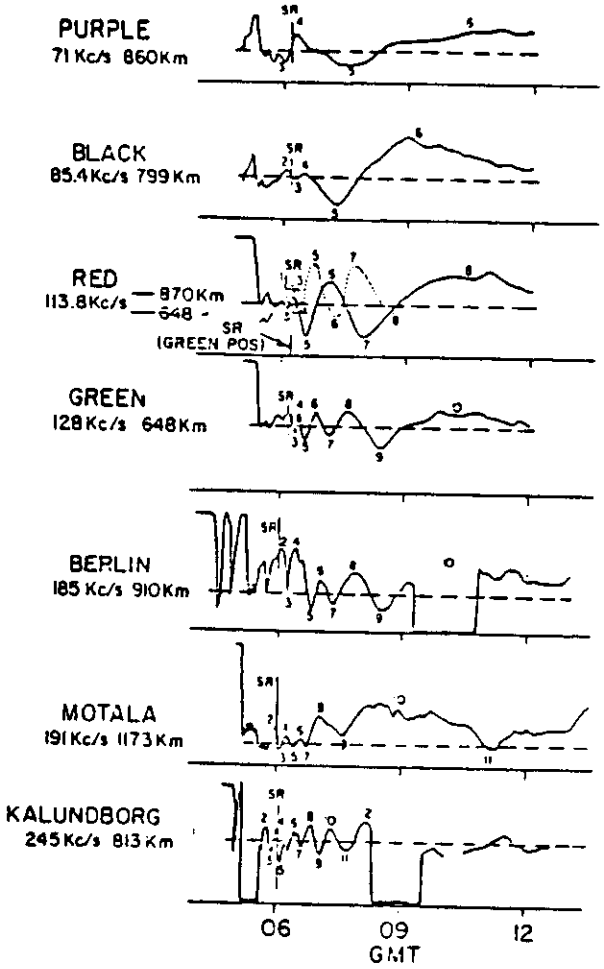

Fig. 7 **Total field** for 11 March 1955 received from range of LF **transmitters** at Cambridge (Dashed line gives estimated **ground-wave** amplitude)

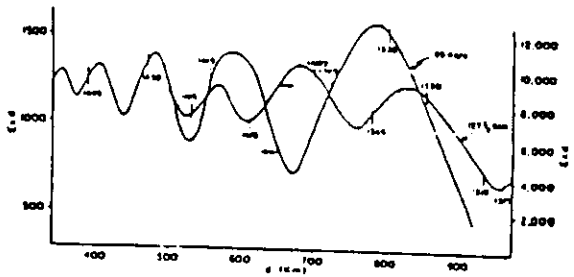

Fig. 8 Hollingsworth interference patterns at 85 and 127½ kHz observed during a flight from Copenhagen to Farnborough on 13 March 1951